


RESEARCH

Open Access



Role of intravoxel incoherent motion MRI in diagnosis and assessment of invasiveness of urothelial bladder carcinoma

Mohamed Ali Badawy¹, Samia Mounir Zaky², Mona S. Korkor^{1*}  and Sherif Abdel Fattah²

Abstract

Background Urinary bladder cancer is a common malignancy. Preoperative accurate judgment of the degree of tissue invasion is crucial to determine the plan of therapy. We aimed in the current study to evaluate the role of intravoxel incoherent motion (IVIM) MRI and apparent diffusion coefficient (ADC) map in differentiating muscle invasive from non-muscle invasive carcinomas.

Results Values of IVIM-derived true diffusion coefficient (D), pseudo-diffusion coefficient (D*) and perfusion fraction (F) and ADC were lower in muscle invasive carcinomas than non-invasive masses with p values < 0.001 and 0.001, respectively. In MIBC, ADC was (0.9×10^{-3} mm²/s), D was (0.8×10^{-3} mm²/s), D* was (6.9×10^{-3} mm²/s) and F was (16.9%). In NMIBC, ADC was (1×10^{-3} mm²/s), D was (1.1×10^{-3} mm²/s), D* was (10.2×10^{-3} mm²/s) and F was (17.7%). Mass D cut off values, sensitivity and specificity and AUC were < 0.9, 83.93, 96.30 and 0.945, respectively. Mass ADC cut off values, sensitivity and specificity and AUC were < 1.09, 87.50, 51.85 and 0.721, respectively. The degree of agreement between IVIM parameters and the pathological staging was assessed by Kappa test. The best agreement was detected for mass D (K=0.796), while the mass ADC and wall beside mass D showed moderate and fair agreement (k=0.418 and 0.325, respectively).

Conclusions IVIM MRI parameters and ADC map can be utilized to detect the degree of tissue invasion caused by bladder cancer.

Keywords Bladder cancer, Muscle invasion, IVIM MRI

Background

Urothelial bladder carcinoma is the fourth most common cancer worldwide in males and ninth one in females. However, It represents the third most common cancer in both genders among Egyptians [1, 2]

Accurate staging of urinary bladder carcinomas using TNM staging system preoperatively is crucial to

determine both the patients prognosis and management plans [3, 4]. It can be classified into either non-muscle-invasive bladder cancers (NMIBC) that includes stage Ta and T1 and is treated with transurethral resection of bladder tumor (TURBT) with or without intravesical instillation of chemotherapy and muscle invasive bladder cancers (MIBC) that includes stages T2–T4 and is treated with radical cystectomy with or without chemotherapy [5].

Although TURBT is the current standard tool to determine the pathological subtype, stage and grade of the tumor [4, 6], it has many limitations as it is relatively an invasive procedure and frequently needs to be repeated with wide variability between urologists [7, 8].

*Correspondence:

Mona S. Korkor
monakorkor2@gmail.com

¹ Diagnostic Radiology and Medical Imaging, Urology and Nephrology Center, Mansoura University, Mansoura, Egypt

² Diagnostic Radiology and Medical Imaging, Faculty of Medicine, Mansoura University, Mansoura, Egypt

The current advancement and availability of multi-parametric magnetic resonance imaging (mp-MRI) techniques provide anatomical information through high-resolution T1 and T2 weighted imaging (WI) in addition to functional information through diffusion-weighted imaging (DWI) and dynamic contrast enhancement (DCE). This allows an accurate evaluation of bladder cancer, staging and grading, before proceeding to invasive cystoscopy [9, 10].

DWI with the calculated apparent diffusion coefficient (ADC), utilizing monoexponential model that depends on the diffusion of water molecules and microcirculation perfusion information, has been used efficiently to determine the degree of invasiveness of bladder cancer [11–13]. After introduction of the intravoxel incoherent motion (IVIM) theory with separation of water molecular diffusion from microcirculation using biexponential model [14], the IVIM-derived true diffusion coefficient (D) reflects water molecular diffusion, pseudo-diffusion coefficient (D*) represents the microvascular portion and the perfusion fraction (f) is related to the fractional volume occupied in the voxel by microvascular flowing spins [15].

Predicting pathological grading using IVIM-MRI has been studied in gliomas, hepatocellular carcinoma, breast cancer, and evaluating the effect of chemotherapy on colorectal carcinoma [15–18]. However, the role of IVIM in bladder cancer is not sufficiently studied; therefore, we conducted the current study to evaluate the use of IVIM derived parameters and ADC values in predicting the invasiveness of bladder urothelial carcinoma and to differentiate MIBC from NMIBC.

Methods

Selection and description of participants

This prospective study was approved by the institutional research and ethical committee of Mansoura University and was approved by the international review board (MS.23.01.2275.RI). Written consents were obtained from all patients prior to examination. It included eighty-three patients with bladder cancer based on clinical suspicion, or ultrasonography findings in the period from January 2023 to July 2023. The study was conducted in Radiology Department (MRI Unit), Urology and Nephrology Center, Mansoura University.

Adequate sample size was calculated using G power program version 3.1.9.4, based on effect size of 0.724, using 2-tailed test, α error=0.05 and power=90.0%, the total calculated sample size was 83 cases. Inclusion criteria: Patients with clinical suspicion of urothelial carcinoma based on clinical suspicion (hematuria, dysuria or frequency) or ultrasound findings (focal thickening of bladder wall, mass protruding into the bladder lumen or

extending into adjacent tissues in advanced cases). Exclusion criteria: Patients with contraindications to MRI study including patients with cardiac pacemaker, metallic implants, or claustrophobic patients or those received neoadjuvant chemotherapy prior to operation and histopathological assessment. Patients who refused to be enrolled in the study and any low image quality or non-standard scan sequences were excluded as illustrated in the flowchart (Fig. 1). Data regarding age, gender, clinical presentation, results of MRI and histopathological examination and operative management of all cases were collected.

Technical information

Regarding MRI examination, all patients were prepared and examined in the supine position using 3-Tesla MRI machine (*Philips Ingenia 3T, Netherlands*) with local phased external array coil (18 channels) put on the patient's abdomen and pelvis. The protocol of MRI examination included high resolution T2WI, DWI with post-processing ADC map (b value=1000) and IVIM-MRI. IVIM-MRI were performed with multiple b values DWI (b values=0, 10, 25, 50, 75, 100, 150, 200, 400, 600, 800, 1000, 1400 s/mm²). Gadolinium-based contrast agents were not used in this study due to high resolution images obtained by 3T scanner and no need for analysis of tissue perfusion in this study.

The available experimental evidence shows that deviation of the diffusion model from Gaussian diffusion appeared as a double exponential form when we increase the range of b-values used. Moreover, it was not clear how high the value of b should be to avoid this deviation in the IVIM model after ignoring the contribution of non-Gaussian diffusion [19]. However, many studies concluded that the error of parameter measurement decreases with increasing the number of b-values used [20]. On the other side, much increase in chosen b values increases the acquisition time and is unrealistic to be applied to avoid possible artifacts and patient intolerance [21]. Therefore, we used 13 b-values in the present study to accurately characterize the nature of the studied lesions, although the plausibility still needs further investigation. The used MRI sequences are illustrated in Table 1.

Regarding the image analysis, all scans were transferred and reviewed on a picture archiving and communication systems (PACS) (Magic View, GE, Milwaukee, WI, USA). T2-WI followed by Diffusion weighted-MR images followed by IVIM sequences—MR images were interpreted referring to T2-WI image sets and the tumors were assigned a T stage in each sequence. When multiple tumors were present, the highest T stage represented the T stage of the patient as follows:

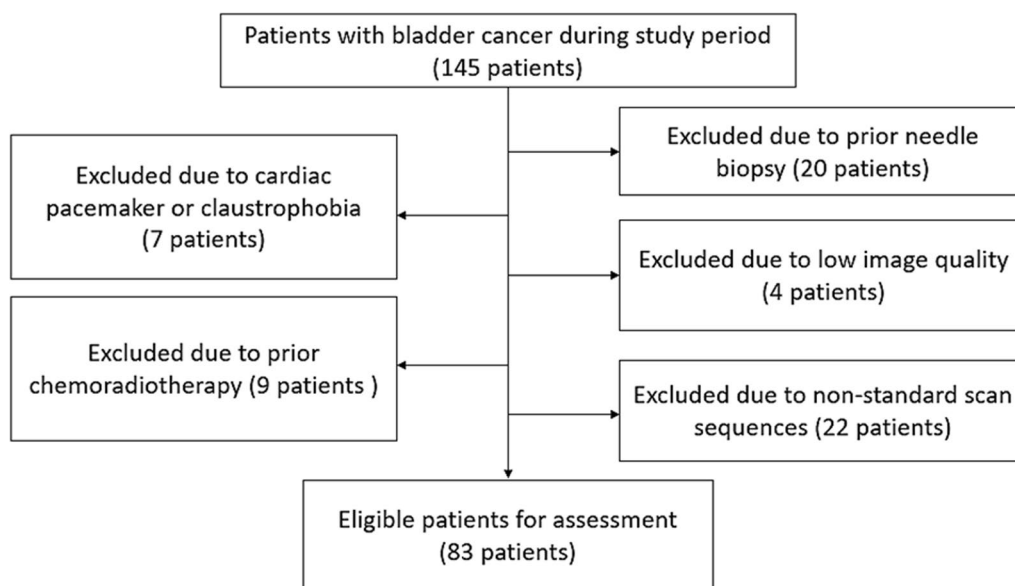


Fig. 1 The flow chart of participants in the present study

Table 1 bpMRI sequences obtained in all patients

MRI protocol	MRI sequences			
	T2WI	DWI	ADC	IVIM
Plane	Axial			
TR (msec)	3800	6430		3050
TE (msec)	80	90		90
Slice thickness (mm)	3	3		3
FOV (cm)	200×190	240×200		230×180
Matrix (mm×mm)	252×257	80×67		76×61
Intersection gap (mm)	0.3	0		0
Number of excitations	2–3	4–10		
b values			0, 1400	0, 10, 25, 50, 75, 100, 150, 200, 400, 600, 800, 1000, 1400

T2WI/T2 weighted image, DWI diffusion weighted image, ADC apparent diffusion coefficient, TR time to repeat, TE time to echo, FOV field of view

Biparametric MRI (bpMRI) and VI-RADS score in bladder cancer

We put tumors scoring using appearances in T2WI, DWI images and IVIM parameters to create an overall risk of invasion score. Normal bladder mucosa/inner layer was not seen on T2WI and DWI sequences; however, they were seen as high SI structures on T2WI images and low SI structures on DWI due to edema or inflammation. Normal muscularis propria showed low SI on T2WI images and DWI.

- a) Qualitative assessment (T2WI and DWI) (Figs. 2 and 3).

1. Assessment for T2WI images: Interruption of the low SI muscular line may suggest muscle invasion. Stage 1: uninterrupted low SI line representing the integrity of muscularis propria (tumor < 1 cm with or without thickened inner layer). Stage 2: uninterrupted low SI line representing the integrity of muscularis propria (tumor > 1 cm with high SI thickened inner layer). Stage 3: uninterrupted low SI line representing the integrity of muscularis propria (tumor > 1 cm without high SI thickened inner layer). Stage 4: interruption of low SI line suggesting extension of the intermediate SI tumor tissue to muscularis propria. Stage 5:

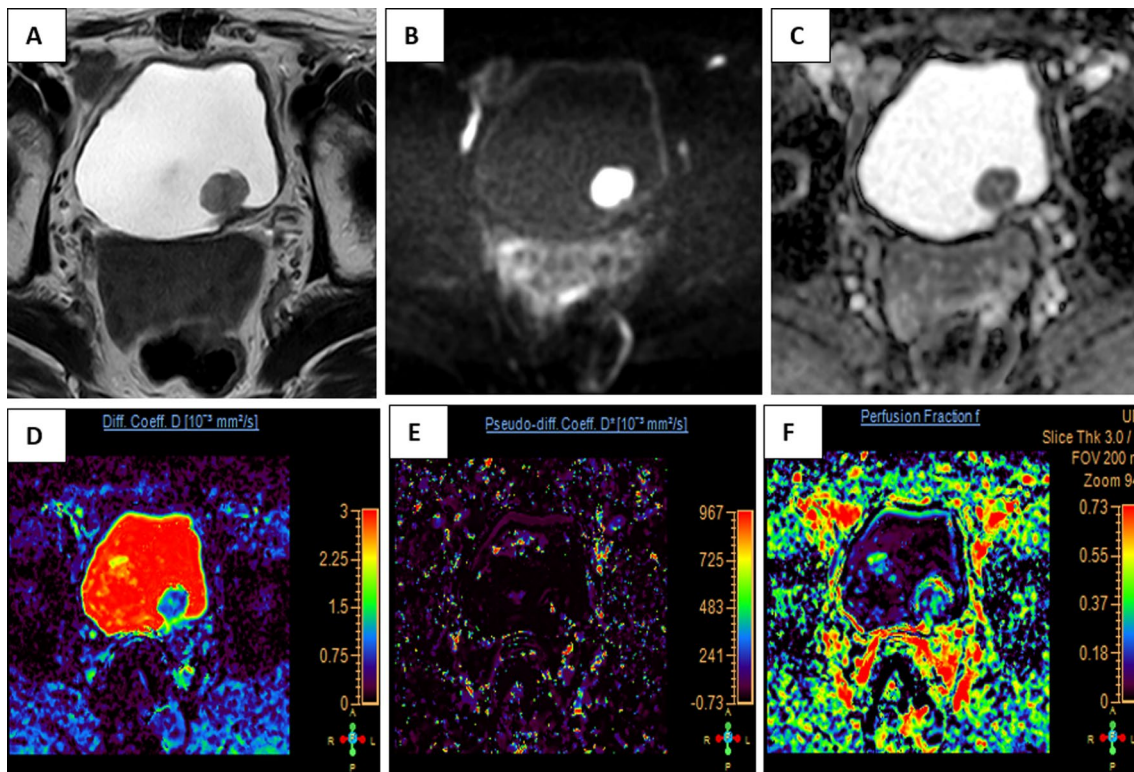


Fig. 2 A 63-year-old male patient presented with NMIBC arising from posterior wall of urinary bladder. **A** Axial T2WI showing small polypoid mass. **B** Axial DWI showing restricted diffusion in the mass with no extension to the perivesical fat ($b=1000 \text{ s/mm}^2$). **C** ADC value of urinary bladder mass = $0.96 \times 10^{-3} \text{ mm}^2/\text{s}$, consistent with low grade bladder carcinoma. **D**, **E** and **F** showing **D**, **D*** and **F** maps with quantitative values were measured as $0.91 \times 10^{-3} \text{ mm}^2/\text{s}$, $5 \times 10^{-3} \text{ mm}^2/\text{s}$ and 0.29, respectively

extension of intermediate SI tumor to extravascular fat, representing the invasion of the entire bladder wall and extravascular structures.

2. Assessment for DWI/ADC map: On DWI, SI of the lesions identified at $b=1000$ images, at these images, the tumor is hyperintense on DWI and hypointense on ADC map. Muscularis propria may present intermediate SI, while the inner layer has low SI on DWI. While analyzing DWI, interpretation was referred to T1 and T2WIs and lesions are classified into: DW category 1: muscularis propria with intermediate continuous SI on DWI (lesion < 1 cm, hyperintense on DWI and hypointense on ADC, with or without low SI thickened inner layer on DWI). DW category 2: muscularis propria with continuous intermediate SI on DWI (lesion > 1 cm, hyperintense on DWI and hypointense on ADC, with low SI thickened inner layer on DWI). DW category 3: muscularis propria with continuous intermediate SI on DWI (lesion > 1 cm, hyperintense on DWI and hypointense on ADC, without SI thickened inner layer on DWI). DW category 4: High SI tumor on

DWI and low SI tumor on ADC extending focally to muscularis propria. DW category 5: High SI tumor on DWI and low SI tumor on ADC extending to the entire bladder wall and extravascular fat.

- b) *Quantitative assessment (ADC value & IVIM parameters)* (Figs. 2 and 3). ADC values were calculated on ADC map by placing region of interest (ROI) on most hypointense areas of the tumors, corresponding normal bladder walls & urine. In addition, the ADC values of wall beside mass were measured. Identification of the pelvic lymph nodes was performed according to their sites. Regarding IVIM parameters: the D , D^* and F were measured and assessed for the mass and wall beside mass (Table 4) in the same way as before using their maps.
- c) *Final scoring* A five-point VI-RADS score is generated using the individual T2WI stage, DWI categories, and IVIM parameters suggesting the probability of muscle invasion: **VI-RADS 1** (muscle invasion is highly unlikely): T2WI Stage I, DW category 1 and ADC, D , D^* and F measure more than (1×10^{-3})

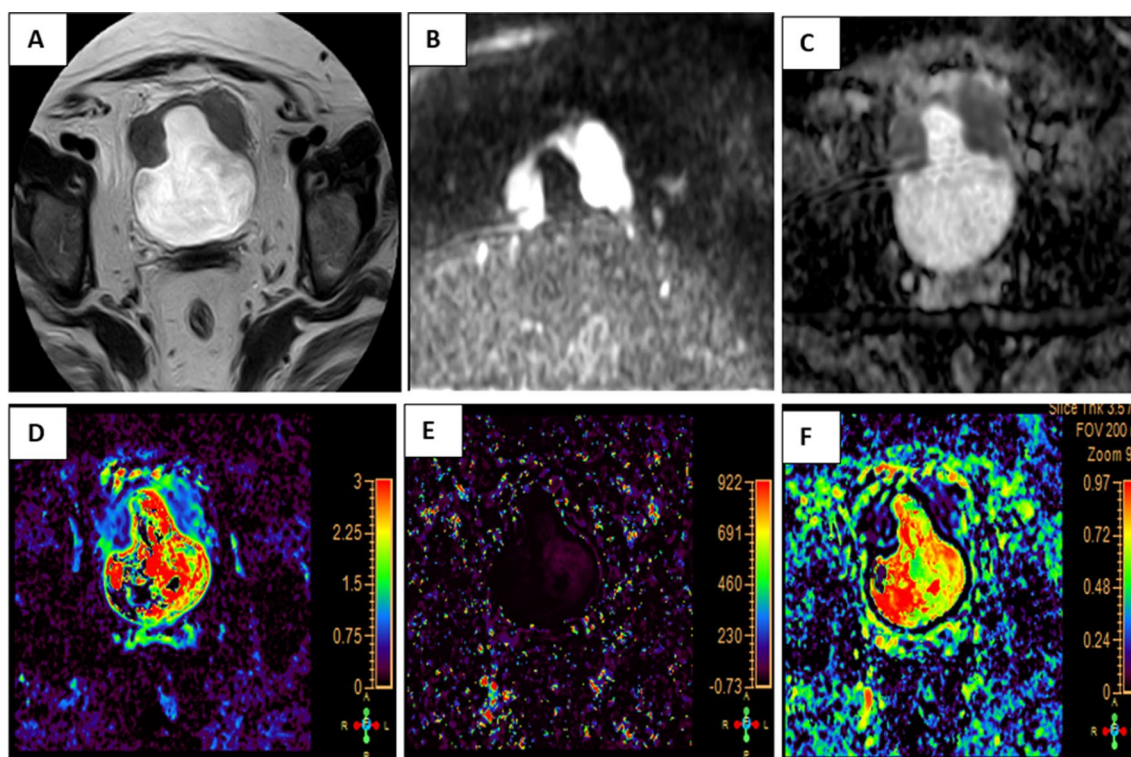


Fig. 3 A 62-year-old female patient with MIBC arising from both anterolateral walls of urinary bladder. **A** Axial T2WI showing two polypoid solid masses. **B** Axial DWI showing restricted diffusion in the masses with infiltration of perivesical fat ($b = 1000 \text{ s/mm}^2$). **C** ADC value of urinary bladder mass = $0.73 \times 10^{-3} \text{ mm}^2/\text{s}$, consistent with high grade bladder carcinoma. **D**, **E** and **F** showing **D**, **D*** and **F** maps with quantitative values were measured as $0.77 \times 10^{-3} \text{ mm}^2/\text{s}$, $5 \times 10^{-3} \text{ mm}^2/\text{s}$ and 0.08, respectively

mm^2/s , $1.1 \times 10^{-3} \text{ mm}^2/\text{s}$, $10.2 \times 10^{-3} \text{ mm}^2/\text{s}$ and 17.7%, respectively). **VI-RADS 2** (muscle invasion is unlikely to be present): T2WI stage 2 and DW category 2 and ADC, D, D* and F measure more than ($1 \times 10^{-3} \text{ mm}^2/\text{s}$, $1.1 \times 10^{-3} \text{ mm}^2/\text{s}$, $10.2 \times 10^{-3} \text{ mm}^2/\text{s}$ and 17.7% respectively). **VI-RADS 3** (the presence of muscle invasion is equivocal): T2WI stage 3 and DW category 3; SC category 3 and ADC, D, D* and F measure about ($1 \times 10^{-3} \text{ mm}^2/\text{s}$, $1.1 \times 10^{-3} \text{ mm}^2/\text{s}$, $10.2 \times 10^{-3} \text{ mm}^2/\text{s}$ and 17.7% respectively). **VI-RADS 4** (muscle invasion is likely): T2WI stage 4 and/or DW category 4 and ADC, D, D* and F measure about ($0.9 \times 10^{-3} \text{ mm}^2/\text{s}$, $0.8 \times 10^{-3} \text{ mm}^2/\text{s}$, $6.9 \times 10^{-3} \text{ mm}^2/\text{s}$ and 16.9% respectively). **VI-RADS 5** (invasion of muscle and beyond the bladder is likely): at least T2 stage 5 plus DW category 5 and ADC, D, D* and F measure less than ($0.9 \times 10^{-3} \text{ mm}^2/\text{s}$, $0.8 \times 10^{-3} \text{ mm}^2/\text{s}$, $6.9 \times 10^{-3} \text{ mm}^2/\text{s}$ and 16.9%, respectively).

Pathological diagnosis

All diagnosed lesions were biopsied either by TURBT or by radical cystectomy and urinary diversion after

diagnostic MRI examinations and underwent histopathological evaluation for definitive diagnosis and assess the degree of muscle invasion, to differentiate MIBC from NMIBC.

Statistics

The collected data was revised, coded, and tabulated using the Statistical package for Social Science (IBM Corp. Released 2017. IBM SPSS Statistics for Windows, Version 25.0. Armonk, NY: IBM Corp.). The normality of data distribution was assessed by Kolmogorov–Smirnov test. Numerical data were presented as either Mean and Standard deviation (\pm SD) or Median and interquartile range (IQR), while non-numerical data were presented as frequency and percentage. Student's t-test was used to compare means of the two studied groups. Mann–Whitney Test (U test) was used to assess the statistical significance of difference of a nonparametric variable between two study groups. Chi-Square test was used to examine the relationship between two qualitative variables.

The ROC curve (receiver operating characteristic) provides a useful way to evaluate the sensitivity and specificity for quantitative diagnostic measures that categorize cases into one of two groups. The optimum cut off point

was defined as that which maximized the AUC value. AUC greater than 0.9 has high accuracy, while 0.7–0.9 indicates moderate accuracy, 0.5–0.7 indicates low accuracy and 0.5 a chance result. The kappa statistic was calculated to estimate agreement between the methods. The strength of agreement of kappa coefficients was guided by the boundaries suggested by Landis and Koch [22]. Values less than 0 indicate "poor" reliability, 0–0.20 is "slight" reliability, 0.21–0.40 is "fair" reliability, 0.41–0.60 is "moderate" reliability, 0.61–0.80 is "substantial" agreement, 0.81–1.00 "excellent" or "almost perfect" agreement. The *p* value is considered significant if <0.05 at confidence interval 95%.

Results

The current study included eighty-three patients with urinary bladder carcinoma. The demographic data, and clinical presentation of the included patients are illustrated in Table 2. The mean age of the studied patients was 65.7 years, and most of the cases (75.9%) were males. Most of the included patients (68.7%) were presented with hematuria, 19.3% had lower urinary tract symptoms, and 12% were accidentally discovered to have bladder cancer during routine ultrasonography.

The radiological assessment of the included patients revealed that the posterior and lateral walls were the most common sites of bladder lesions. Most patients (53%) had a single lesion with the polypoid fungating mass as the most common morphology of encountered lesions (77.1%). The most common radiological stage observed was T2 (33.7% of the cases). In terms of lymph node involvement (N), the most prevalent stage was N0 (78.3% of the cases) and most of the cases (97.6%) exhibit no distant metastasis (M0). Most cases (54.2%) underwent TURBT. The mean time of operation was 12.6 ± 11.4 days after MRI as shown in Table 3.

Table 2 Demographic and clinical characteristics of the studied patients

Variable		Total patients (N=83)
Age (years)	M \pm SD	65.7 \pm 11.9
	Median (IQR)	67 (20–86)
Gender		
Male	N (%)	63 (75.9%)
Female	N (%)	20 (24.1%)
Clinical presentation		
Hematuria	N (%)	57 (68.7%)
Lower urinary tract symptoms	N (%)	16 (19.3%)
Accidentally discovered	N (%)	10 (12%)

N number, % percentage, SD standard deviation, IQR interquartile range, N (%): number (percentage)

Regarding the pathological results of the performed biopsies, the most common pathological type was transitional/urothelial carcinoma (86.7%), followed by squamous cell carcinoma (13.3%). Most patients (79.5%) had high grade of carcinoma while the most common pathological stage (T) observed in the provided data was T2 (31.3% of the cases). In terms of lymph node involvement (N), the most prevalent stage was N0 (81.9% of the cases). Additionally, most of the cases (95.2%) had no evidence of distant metastasis (M0). Among the cases, 67.5% were classified as Muscle-invasive bladder cancer (MIBC) including those with stage T2 or more, while 32.5% were categorized as non-muscle-invasive bladder cancer (NMIBC) including stage T1. Hence, the included patients were further subdivided into two groups MIBC and NMIBC as in Table 3.

Significant differences between the studied groups were observed in the type and the time of operation after MRI performance. All patients in the NMIBC group underwent TURBT, while most patients in the MIBC group (67.9%) underwent radical cystectomy ($p < 0.001$). Regarding the time of operation after MRI performance, the MIBC group had a significantly longer waiting period compared to the NMIBC group ($p = 0.015$). According to the pathology of performed biopsies in both groups, MIBC group had a higher proportion of high-grade tumors (87.5%) compared to the NMIBC group (63%), with ($p = 0.009$) (Table 3).

The IVIM MRI and ADC parameters were evaluated in all included patients and then compared between both studied groups. The mass D, mass ADC and wall beside mass D values were significantly lower among MIBC group compared to the NMIBC group, with (*p* values < 0.001 , 0.001 and 0.006), respectively. In MIBC, mass ADC (0.9×10^{-3} mm²/s), mass D (0.8×10^{-3} mm²/s), mass D* (6.9×10^{-3} mm²/s) and mass F (16.9%). In NMIBC, ADC (1×10^{-3} mm²/s), D (1.1×10^{-3} mm²/s), D* (10.2×10^{-3} mm²/s) and F (17.7%) (Table 4 and Fig. 4).

ROC curve analysis was performed for discrimination between the two studied groups according to MRI-IVIM and ADC parameters. While mass D showed high accuracy (AUC=0.945), the mass ADC showed moderate accuracy (AUC=0.721). However, the wall beside mass D showed low accuracy (AUC=0.686), for discrimination between NMIBC from MIBC. Mass D cut off values, sensitivity and specificity were < 0.9 , 83.93 and 96.30, respectively. Mass ADC cut off values, sensitivity and specificity were < 1.09 , 87.50 and 51.85, respectively (Table 5 and Fig. 5).

The degree of agreement between the bpMRI and pathological staging was evaluated by the Kappa agreement as shown in Table 6 and Fig. 6. As regards T stages, they were 55.6%, 53.8%, 80.0% and 70.0% for stages T1,

Table 3 MRI and pathological characteristics of the studied patients

Variable		Total patients (N=83)
<i>MRI assessment of the lesions</i>		
Site of the mass		
Anterior wall	N (%)	19 (22.9%)
Posterior wall	N (%)	32 (38.6%)
Lateral wall	N (%)	24 (28.9%)
Circumferential	N (%)	8 (9.6%)
Number of the lesions		
Single	N (%)	44 (53%)
Multicentric	N (%)	39 (47%)
Morphology of the lesion		
Superficial nodular growth	N (%)	15 (18.1%)
Fungating mass	N (%)	64 (77.1%)
Diffuse mural thickening	N (%)	4 (4.8%)
bpMRI stage of the tumor (T)		
1	N (%)	20 (24.1%)
2	N (%)	28 (33.7%)
3	N (%)	24 (28.9%)
4	N (%)	11 (13.3%)
bpMRI stage (N)		
0	N (%)	65 (78.3%)
1	N (%)	10 (12%)
2	N (%)	6 (7.2%)
3	N (%)	2 (2.4%)
bpMRI stage (M)		
0	N (%)	81 (97.6%)
1	N (%)	2 (2.4%)
<i>Surgical details of the studied patients</i>		
Type of operation		
TURBT	N (%)	45 (54.2%)
Radical cystectomy	N (%)	38 (45.8%)
Time of operation after MRI performance (days)	M ± SD	12.6 ± 11.4
	Median (IQR)	10 (1–30)
Pathological type		
Transitional/ urothelial carcinoma	N (%)	72 (86.7%)
Squamous cell carcinoma	N (%)	11 (13.3%)
<i>Pathological characteristics of the lesions</i>		
Grade		
Low	N (%)	17 (20.5%)
High	N (%)	66 (79.5%)
Pathological stage (T)		
1	N (%)	27 (32.5%)
2	N (%)	26 (31.3%)
3	N (%)	20 (24.1%)
4	N (%)	10 (12%)
Pathological stage (N)		
0	N (%)	68 (81.9%)
1	N (%)	7 (8.4%)
2	N (%)	8 (9.6%)

Table 3 (continued)

Variable		Total patients (N = 83)
Pathological stage (M)		
0	N (%)	79 (95.2%)
1	N (%)	4 (4.8%)
Muscle invasion		
MIBC	N (%)	56 (67.5%)
NMIBC	N (%)	27 (32.5%)

N number, %: percentage, SD standard deviation, IQR interquartile range, T tumor stage, N lymph node involvement, M distant metastasis, TURBT transurethral resection of bladder tumor, MRI magnetic resonant imaging, MIBC muscle invasive bladder cancer, NMIBC non-muscle invasive bladder cancer, N(%): number (percentage)

Table 4 bpMRI parameters (IVIM and ADC) in the studied groups

Variable	MIBC (N = 56)	NMIBC (N = 27)	Test	p value
Mass D ($\times 10^{-3}$ mm ² /s)	0.8 \pm 0.1	1.1 \pm 0.1	Z=6.910	<0.001*
Mass D* ($\times 10^{-3}$ mm ² /s)	6.9 \pm 3.4	10.2 \pm 8.9	Z=1.564	0.118
Mass F (%)	16.9 \pm 8.9	17.7 \pm 9.7	Z=0.170	0.865
Mass ADC ($\times 10^{-3}$ mm ² /s)	0.9 \pm 0.2	1 \pm 0.2	Z=3.248	0.001*
Wall beside mass D ($\times 10^{-3}$ mm ² /s)	0.9 \pm 0.2	1.1 \pm 0.4	Z=2.728	0.006*
Wall beside mass D* ($\times 10^{-3}$ mm ² /s)	8.8 \pm 6.9	13.7 \pm 12.5	Z=1.570	0.116
Wall beside F (%)	23.4 \pm 13.8	18.6 \pm 13.6	Z=1.416	0.157
wall beside mass ADC ($\times 10^{-3}$ mm ² /s)	1 \pm 0.2	1.1 \pm 0.2	Z=0.554	0.579

MIBC muscle invasive bladder cancer, NMIBC non-muscle invasive bladder cancer, MRI magnetic resonant imaging, IVIM Intravoxel Incoherent Motion, D true diffusion coefficient, D* pseudo-diffusion coefficient, ADC apparent diffusion coefficient standard, f perfusion fraction, Z = Mann Whitney test; *p < 0.05

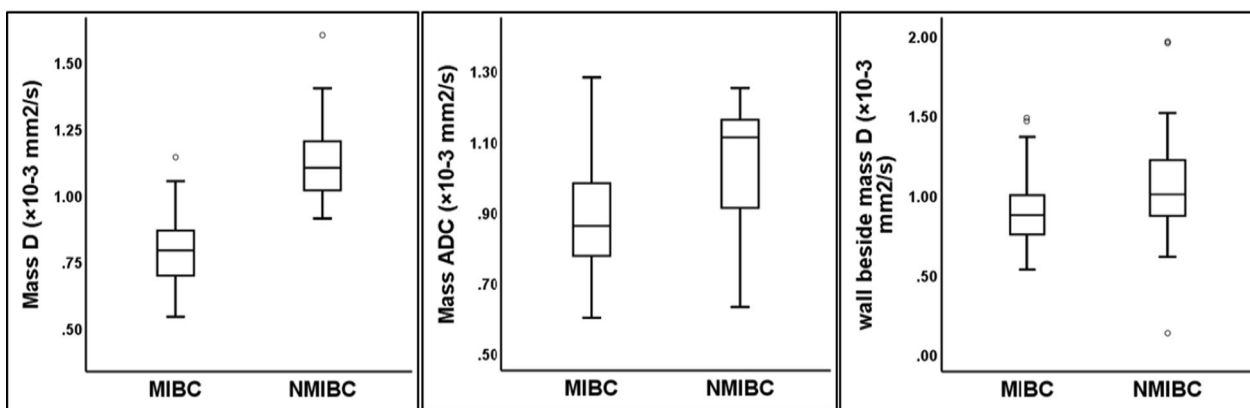


Fig. 4 Boxplots show the difference between MIBC and NMIBC according to the Mass D, ADC, and wall beside mass D in the studied groups with P values < 0.001, 0.001 and 0.006, respectively. MIBC muscle invasive bladder cancer, NMIBC non-muscle invasive bladder cancer, D true diffusion coefficient, ADC apparent diffusion coefficient standard

T2, T3 and T4, respectively, with a kappa agreement value of 0.489, indicating a moderate overall agreement in T staging. While the degree of agreement in N stages revealed that N0, N1, N2 and N3 had agreement percentages of 82.4%, 42.9%, 25.0% and 0.0%, respectively, with a kappa agreement value of 0.223, indicating a fair overall agreement in N staging. For the M stages, the agreement

percentage for M0 and M1 were 97.5%, and 0.0%, respectively, with a kappa agreement value of -0.033, indicating a slight disagreement between radiology and pathology staging for M stages. Furthermore, the degree of agreement between IVIM parameters and the pathological staging was evaluated by Kappa test. The best agreement was detected for mass D, substantial agreement

Table 5 Results of the ROC analyses for discriminating NMIBC from MIBC

Variable	AUC	95% CI	p value	Cut off	Sensitivity (%)	Specificity (%)
Mass D	0.945	0.873 to 0.983	<0.001*	<0.9	83.93	96.30
Mass ADC	0.721	0.612 to 0.814	0.003*	<1.09	87.50	51.85
Wall beside mass D	0.686	0.574 to 0.783	0.004*	<0.97	71.43	62.96

MIBC muscle invasive bladder cancer, NMIBC non-muscle invasive bladder cancer, ROC receiver operating characteristic, AUC area under ROC curve, CI confidence interval, *Significant <0.05

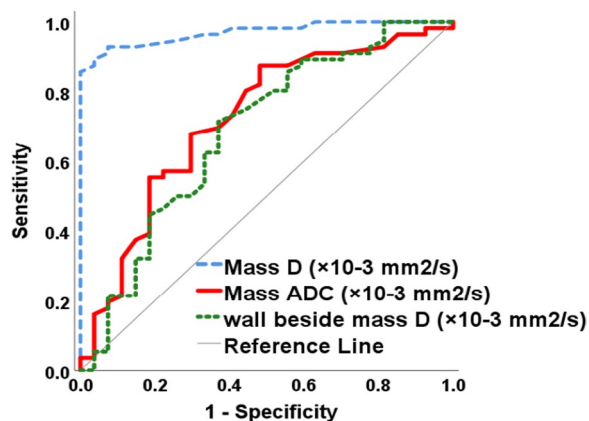


Fig. 5 ROC curve of Mass D, ADC and wall beside mass D for Discriminating MIBC From NMIBC. MIBC muscle invasive bladder cancer, NMIBC non-muscle invasive bladder cancer, ROC receiver operating characteristic, AUC area under ROC curve, CI confidence interval, *Significant <0.05

(K=0.796), while the mass ADC and wall beside mass D showed moderate and fair agreement (k=0.418 and 0.325, respectively).

Discussion

Bladder cancer is the sixth most common cancer [23]. The main classification for bladder cancers is NMIBC vs. MIBC [24]. Cystoscopy is the commonest tool for diagnosing and treating bladder cancer, allowing direct access to a tumor for biopsy and/or resection [25]. The standard

treatment is transurethral resection for NMIBC and radical cystectomy and neoadjuvant chemotherapy for MIBC [26].

The differentiation between MIBC and NMIBC is crucial. It determines the plan of therapy as well as the patient’s prognosis. So, we conducted the current study to evaluate the value of IVIM MRI parameters and ADC values in differentiating MIBC and NMIBC as the data available regarding IVIM in bladder cancer is limited.

This study was conducted on eighty-three patients with urinary bladder carcinoma. All included cases underwent TURBT as diagnostic and therapeutic intervention for NMIBC and diagnostic one for MIBC before proceeding to radical cystectomy and either ileal loop conduit or W-shaped ileal orthotopic neobladder. The pathological staging in our cohort revealed that NMIBC (stage 1) was presented in 32.5% of the cases, while MIBC (stage 2 or more) represented 67.5% of the cases. Forty-five (54.2%) patients operated by TURBT and thirty-eight patient (45.8%) by radical cystectomy,

MRI differentiates the bladder wall layers and enables an accurate assessment of the depth of tumor invasion and extravesical extension [27]. MRI provides anatomical and physiological images for qualitative evaluation and allows for the measurement of model-based quantitative parameters [28]. Quantitative parameters derived from DWI enable numerical values that promise improvements in detecting, staging, and evaluating treatment response in bladder cancer [29]. DWI-derived parameters include the apparent diffusion

Table 6 Agreement between IVIM parameters and pathological staging

IVIM parameters	Pathology				Kappa agreement	Test	
	MIBC (N = 56)		NMIBC (N = 27)				
	N	%	N	%			
Mass D <0.9	48	85.7	0	0.0	K=0.796	54.88	<0.001*
Mass ADC <1.09	49	87.5	13	48.1	K=0.418	14.92	<0.001*
wall beside mass D <0.97	40	71.4	10	37.0	K=0.325	8.99	0.003*

MIBC muscle invasive bladder cancer, NMIBC non-muscle invasive bladder cancer, MRI magnetic resonant imaging, IVIM Intravoxel Incoherent Motion, D true diffusion coefficient, ADC apparent diffusion coefficient standard, χ^2 = chi-square test; *p <0.05

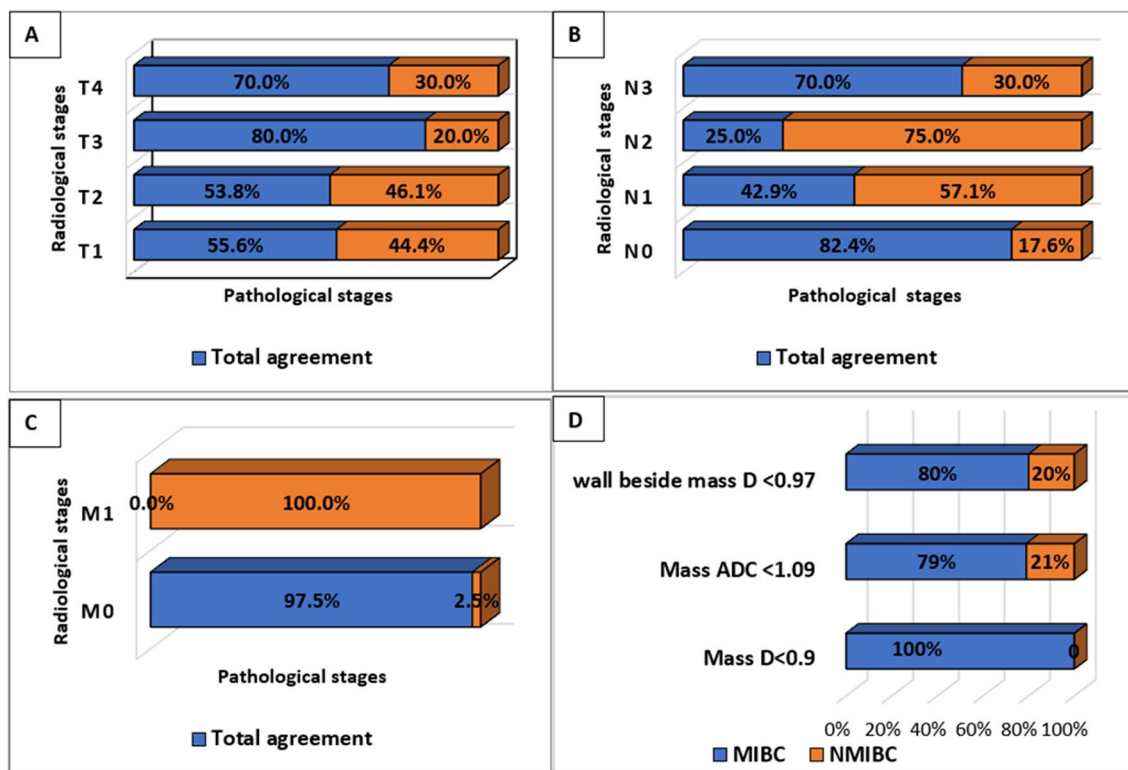


Fig. 6 Degree of agreement between bpMRI and pathological staging. **A** degree of agreement between radiological and pathological T staging, **B** agreement in N staging, **C** degree of agreement in M staging, **D** agreement between significant IVIM parameters and pathological staging. MIBC muscle invasive bladder cancer, NMIBC non-muscle invasive bladder cancer, D true diffusion coefficient, ADC apparent diffusion coefficient standard

coefficient (ADC, the composite of both diffusion and capillary perfusion) and true diffusion coefficient (D, capturing tumor cellularity, extracellular-space tortuosity, and integrity of cellular membranes) [30]. The acquisition, interpretation, and reporting of mpMRI for bladder cancer were standardized by Vesical Imaging-Reporting and Data System (VI-RADS) [31]. VI-RADS’s scoring comprises T2-WI, DWI, and DCE-MRI as a qualitative assessment for diagnostic reporting [32]. The dominant MRI sequence for bladder cancer risk assessment is DWI. If DWI-MRI is suboptimal, DCE-MRI is considered a second option [32].

In our study, we used T2WI and IVIM MRI in biparametric MRI protocol for staging of urinary bladder carcinoma (VI-RADS). T2WI and DWI were used for qualitative evaluation, ADC values and IVIM parameter (D, D* & F) were used for quantitative evaluation. We found that the moderate overall agreement between radiological and pathological staging of the tumor in addition to the substantial agreement between mass D value and pathological classification. This indicates that IVIM parameters especially mass D value is a valuable tool to predict the aggressiveness of bladder cancer and can guide the plan of therapy.

Regarding IVIM parameters, we found that MIBC had lower values of mass D and wall beside mass D compared to NMIBC, with p values < 0.001 and 0.006, respectively. Moreover, in the context of ADC values, MIBC had lower ADC values than NMIBC. However, the D* and f values did not differ between both groups. Regarding the sensitivity and specificity of different IVIM parameters, the D value has significantly larger AUC than that of ADC. The D value has 83.93% sensitivity and 96.3% specificity while ADC has 87.5% sensitivity and 51.85% specificity. The best combination of parameters was combined D and ADC values.

In line with our results, Wang et al. reported that the ADC and D value were significantly lower in patients with MIBC compared to those with NMIBC (P < 0.01). No significant differences were observed in D* and f. The AUC of D value (0.894) was significantly larger than the ADC value (0.786), with sensitivities and specificities of 95% and 87.5% for (D) and 80% and 68.7% for (ADC), respectively. In addition, the D and ADC values were significantly correlated with Ki-67 LI (r = -0.785, r = -0.643, respectively; both P < 0.01) [33].

We agree with Akin et al. who reported that Qualitative and quantitative MRI offer excellent contrast resolution

for preoperative staging for bladder cancer [34]. Also, we agree with Johi et al. who suggested that adding DWI-derived parameters to T2WI improves the accuracy of MRI in bladder cancer detection and staging; staging accuracy was better in T2WI plus DWI-MRI (83%) as compared to DW-MRI alone (77%) or T2WI alone (75%) [34].

In contrary to our results, Zhang et al., reported that the ADC and D values differed significantly among low, intermediate, and high-aggressive urothelial bladder carcinomas ($P < 0.05$). However, the f values showed significant difference when compared between low and high-aggressive or intermediate and high-aggressive bladder carcinomas ($P < 0.05$). The best parameter for differentiating high from low/intermediate aggressive urothelial bladder carcinoma was ADC value, with the AUC and accuracy of 0.895 and 85.97%, respectively. Moreover, the f and D values had AUCs of 0.873 and 0.862, respectively. The best differentiating parameter was combination of D and f values, with AUC of 0.931 and 91.82%, accuracy [35].

Limitations of the current study

There are some limitations of the present study as being a single center study and obtaining the analyzed parameters from single region of interest (ROI) that may not fully reflect the information of the whole tumor. Moreover, we did not use IV contrast, so our research is considered biparametric not multi-parametric study, and the sample size is comparatively small. In addition, MRI examination may be amenable to patient motion or bladder catheter artifacts which were encountered in few cases. Despite these limitations, our results provide important new insight into the emerging role of IVIM-MRI in diagnosis and staging of UB carcinoma.

Conclusions

IVIM MRI and ADC can add more information in evaluation of bladder cancer. They can help in staging and grading of bladder cancer as well as their precious role in follow up and thus combination of such functional sequences should be advocated whenever differentiation between superficial and muscle invasive disease during preoperative workup and post-operative follow up is required. Mass D showed higher accuracy for discrimination between NMIBC From MIBC than Mass ADC. The best cut-off values and performance characteristics of mass D, mass ADC and wall beside mass D were < 0.9 , < 1.09 and < 0.97 , respectively. Although the current study included quite enough cases, further multicenter studies on larger sample size may be beneficial to confirm our data.

Abbreviations

ADC	Apparent diffusion coefficient
bpMRI	Biparametric MRI
D	True diffusion coefficient
D*	Pseudodiffusion coefficient
DWI	Diffusion-weighted imaging
DCE	Dynamic contrast enhancement
f	Perfusion fraction
IVIM	Intravoxel incoherent motion
MIBC	Muscle-invasive bladder cancers
MRI	Magnetic resonant imaging
NMIBC	Non-muscle-invasive bladder cancers
ROI	Region of interest
TURBT	Transurethral resection of bladder tumor

Acknowledgements

We acknowledge all members of the Radiology Department in Urology and Nephrology Center, Mansoura University, Egypt.

Author contributions

M.K. contributed to the data collection. M.K. and M.B. performed data analysis and writing. M.B., S.Z. and S.A. performed supervision. They all approved the final version of the manuscript.

Funding

No funding resources were received for the current study.

Availability of data and materials

The datasets used and/or analyzed are available from the corresponding author on reasonable request.

Declarations

Ethics approval and consent to participate

This study was approved by the Research Ethics Committee of the Faculty of Medicine at Mansoura University in Egypt on 30/01/2023; reference number of approval: (MS.23.01.2275.R1).

Consent for participation

Informed consent was obtained from all patients prior to inclusion in the study.

Consent for publication

Not applicable (no identifying information about participants is available in the article).

Competing interests

The authors declare that they have no competing interests.

Received: 10 October 2023 Accepted: 5 February 2024

Published online: 20 February 2024

References

- Kumar N, Talwar R, Nandy PR (2017) Efficacy of voided urinary cytology and ultrasonography compared to cystoscopy in the detection of urinary bladder cancer. *African Journal of Urology* 23(3):192–196
- Moussa S, El-Sheshtawy W (2017) Pathological pattern of urinary bladder cancer: data from a single Egyptian Institute. *Res Oncol* 13(1):14–17
- Martingano P, Stacul F, Cavallaro M, Casagrande F, Cernic S, Belgrano M et al (2010) 64-Slice CT urography: 30 months of clinical experience. *Radiol Med (Torino)* 115(6):920–935
- Richards KA, Smith ND, Steinberg GD (2014) The importance of transurethral resection of bladder tumor in the management of nonmuscle invasive bladder cancer: a systematic review of novel technologies. *J Urol* 191(6):1655–1664

5. Milowsky MI, Rumble RB, Booth CM, Gilligan T, Eapen LJ, Hauke RJ et al (2016) Guideline on muscle-invasive and metastatic bladder cancer (European Association of Urology guideline): American Society of Clinical Oncology clinical practice guideline endorsement. *J Clin Oncol* 34(16):1945–1952
6. Wang H, Pui MH, Guo Y, Li S, Guan J, Zhang X et al (2015) Multiparametric 3-T MRI for differentiating low-versus high-grade and category T1 versus T2 bladder urothelial carcinoma. *Am J Roentgenol* 204(2):330–334
7. Shariat SF, Palapattu GS, Karakiewicz PI, Rogers CG, Vazina A, Bastian PJ et al (2007) Discrepancy between clinical and pathologic stage: impact on prognosis after radical cystectomy. *Eur Urol* 51(1):137–151
8. Takeuchi M, Sasaki S, Naiki T, Kawai N, Kohri K, Hara M et al (2013) MR imaging of urinary bladder cancer for T-staging: a review and a pictorial essay of diffusion-weighted imaging. *J Magn Reson Imaging* 38(6):1299–1309
9. Gupta N, Sureka B, Kumar MM, Malik A, Bhushan TB, Mohanty NJ (2015) Comparison of dynamic contrast-enhanced and diffusion weighted magnetic resonance image in staging and grading of carcinoma bladder with histopathological correlation. *Urol Ann* 7(2):199
10. Badawy M, Farg H, Gadelhak B, ElGhar MA, Sadeq AG, Borg MJ et al (2020) Diagnostic performance of 3-tesla multiparametric MRI for assessment of the bladder cancer t stage and histologic grade. *Egypt J Radiol Nucl Med* 51(1):1–11
11. El-Assmy A, Abou-El-Ghar ME, Mosbah A, El-Nahas AR, Refaie HF, Hekal IA et al (2009) Bladder tumour staging: comparison of diffusion-and T2-weighted MR imaging. *Eur Radiol* 19(7):1575–1581
12. Yoshida S, Koga F, Masuda H, Fujii Y, Kihara KJ (2014) Role of diffusion-weighted magnetic resonance imaging as an imaging biomarker of urothelial carcinoma. *Int J Urol* 21(12):1190–1200
13. Lin W-C, Chen J-H (2015) Pitfalls and limitations of diffusion-weighted magnetic resonance imaging in the diagnosis of urinary bladder cancer. *Transl Oncol* 8(3):217–230
14. Le Bihan D, Breton E, Lallemand D, Aubin M, Vignaud J, Laval-Jeantet MJR (1988) Separation of diffusion and perfusion in intravoxel incoherent motion MR imaging. *Radiology* 168(2):497–505
15. Shen N, Zhao L, Jiang J, Jiang R, Su C, Zhang S et al (2016) Intravoxel incoherent motion diffusion-weighted imaging analysis of diffusion and microperfusion in grading gliomas and comparison with arterial spin labeling for evaluation of tumor perfusion. *J Magn Reson Imaging* 44(3):620–632
16. Granata V, Fusco R, Catalano O, Guarino B, Granata F, Tatangelo F et al (2016) Intravoxel incoherent motion (IVIM) in diffusion-weighted imaging (DWI) for Hepatocellular carcinoma: correlation with histologic grade. *Oncotarget* 7(48):79357
17. Yuan J, Wong OL, Lo GG, Chan HH, Wong TT, Cheung PS et al (2016) Statistical assessment of bi-exponential diffusion weighted imaging signal characteristics induced by intravoxel incoherent motion in malignant breast tumors. *Quant Imaging Med Surg* 6(4):418
18. Zhu HB, Zhang XY, Zhou XH, Li XT, Liu YL, Wang S et al (2017) Assessment of pathological complete response to preoperative chemoradiotherapy by means of multiple mathematical models of diffusion-weighted MRI in locally advanced rectal cancer: a prospective single-center study. *J Magn Reson Imaging* 46(1):175–178
19. Pang Y, Turkbey B, Bernardo M, Kruecker J, Kadoury S, Merino MJ et al (2013) Intravoxel incoherent motion MR imaging for prostate cancer: an evaluation of perfusion fraction and diffusion coefficient derived from different b-value combinations. *Magn Reson Med* 69(2):553–562
20. Malagi AV, Das CJ, Khare K, Calamante F, Mehndiratta A (2019) Effect of combination and number of b values in IVIM analysis with post-processing methodology: simulation and clinical study. *Magn Reson Mater Phys Biol Med* 32:519–527
21. Pan J, Zhang H, Man F, Shen Y, Wang Y, Zhong Y et al (2018) Measurement and scan reproducibility of parameters of intravoxel incoherent motion in renal tumor and normal renal parenchyma: a preliminary research at 30 T MR. *Abdom Radiol* 43:1739–1748
22. Landis JR, Koch GG (1977) The measurement of observer agreement for categorical data. *Biometrics* 1977:159–174
23. Siegel RL, Miller KD, Wagle NS, Jemal A (2023) Cancer statistics, 2023. *Ca Cancer J Clin* 73(1):17–48
24. Robertson AG, Kim J, Al-Ahmadie H, Bellmunt J, Guo G, Cherniack AD et al (2017) Comprehensive molecular characterization of muscle-invasive bladder cancer. *Cell* 171(3):540–556
25. Tholomier C, Souhami L, Kassouf W (2020) Bladder-sparing protocols in the treatment of muscle-invasive bladder cancer. *Transl Androl Urol* 9(6):2920
26. Tanaka H, Kijima T, Fujii Y (2020) Bladder preservation therapy in muscle-invasive bladder cancer: Current evidence and future perspectives. *AME Med J*
27. Li Q, Cao B, Tan Q, Liu K, Jiang S, Zhou J (2021) Prediction of muscle invasion of bladder cancer: a comparison between DKI and conventional DWI. *Eur J Radiol* 136:109522
28. Donaldson SB, Bonington SC, Kershaw LE, Cowan R, Lyons J, Elliott T et al (2013) Dynamic contrast-enhanced MRI in patients with muscle-invasive transitional cell carcinoma of the bladder can distinguish between residual tumour and post-chemotherapy effect. *Eur J Radiol* 82(12):2161–2168
29. Panebianco V, Narumi Y, Altun E, Bochner BH, Efsthathiou JA, Hafeez S et al (2018) Multiparametric magnetic resonance imaging for bladder cancer: development of VI-RADS (Vesical Imaging-Reporting And Data System). *Eur Urol* 74(3):294–306
30. Panebianco V, Narumi Y, Barchetti G, Montironi R, Catto JWF (2019) Should we perform multiparametric magnetic resonance imaging of the bladder before transurethral resection of bladder? Time to reconsider the rules. *Eur Urol* 76(1):57–58
31. Panebianco V, Pecoraro M, Del Giudice F, Takeuchi M, Muglia VF, Messina E et al (2022) VI-RADS for bladder cancer: current applications and future developments. *J Magn Reson Imaging* 55(1):23–36
32. Zhang X, Wang Y, Zhang J, Zhang L, Wang S, Chen Y (2022) Development of a MRI-based radiomics nomogram for prediction of response of patients with muscle-invasive bladder cancer to neoadjuvant chemotherapy. *Front Oncol* 12:878499
33. Wang F, Wu LM, Hua XL, Zhao ZZ, Chen XX, Xu JR (2018) Intravoxel incoherent motion diffusion-weighted imaging in assessing bladder cancer invasiveness and cell proliferation. *J Magn Reson Imaging* 47(4):1054–1060
34. Al Johi RS, Seifeldin GS, Moeen AM, Aboulhagag NA, Moussa EM, Hameed DA et al (2018) Diffusion weighted magnetic resonance imaging in bladder cancer, is it time to replace biopsy? *Central Eur J Urol* 71(1):31
35. Zhang M, Chen Y, Cong X, Zhao X (2018) Utility of intravoxel incoherent motion MRI derived parameters for prediction of aggressiveness in urothelial bladder carcinoma. *J Magn Reson Imaging* 48(6):1648–1656

Publisher's Note

Springer Nature remains neutral with regard to jurisdictional claims in published maps and institutional affiliations.